

Biofuel Cell Controlled by Enzyme Logic Systems

Liron Amir,^{†,‡} Tsz Kin Tam,[†] Marcos Pita,[†] Michael M. Meijler,[§] Lital Alfonta,^{*,‡} and Evgeny Katz^{*,†}

Department of Chemistry and Biomolecular Science, and NanoBio Laboratory (NABLAB), Clarkson University, Potsdam, New York 13699-5810, and Departments of Biotechnology Engineering and Chemistry, Ben-Gurion University of the Negev, Beer-Sheva 84105, Israel

Received October 6, 2008; E-mail: ekatz@clarkson.edu; alfonta@bgu.ac.il

Abstract: An enzyme-based biofuel cell with a pH-switchable oxygen electrode, controlled by enzyme logic operations processing in situ biochemical input signals, has been developed. Two Boolean logic gates (**AND/OR**) were assembled from enzyme systems to process biochemical signals and to convert them logically into pH-changes of the solution. The cathode used in the biofuel cell was modified with a polymer-brush functionalized with Os-complex redox species operating as relay units to mediate electron transport between the conductive support and soluble laccase biocatalyzing oxygen reduction. The electrochemical activity of the modified electrode was switchable by alteration of the solution pH value. The electrode was electrochemically mute at pH > 5.5, and it was activated for the bioelectrocatalytic oxygen reduction at pH < 4.5. The sharp transition between the inactive and active states was used to control the electrode activity by external enzymatic systems operating as logic switches in the system. The enzyme logic systems were decreasing the pH value upon appropriate combinations of the biochemical signals corresponding to the **AND/OR** Boolean logic. Then the pH-switchable electrode was activated for the oxygen reduction, and the entire biofuel cell was switched ON. The biofuel cell was also switched OFF by another biochemical signal which resets the pH value to the original neutral value. The present biofuel cell is the first prototype of a future implantable biofuel cell controlled by complex biochemical reactions to deliver power on-demand responding in a logical way to the physiological needs.

Introduction

Biofuel cells based on purified enzymes or whole microbial cells are promising future alternative sources of sustainable electrical energy.¹ They include two bioelectrocatalytic electrodes: one for oxidation of organic compounds² and another for reduction of oxygen.³ Enzymes⁴ or microbial cells⁵ are used to biocatalyze redox transformations at the electrodes and/or generate oxidizable substrates from raw organic substances. In

the last 10–15 years the fundamental problems of coupling between the biochemical and electrochemical processes, mostly related to the efficient interfacial charge transport using mediated or direct electron transfer between enzymes and electrodes, were solved⁶ and the biofuel cells became feasible.⁷ However, their practical applications still require solutions of many difficult engineering problems, particularly related to their long-term operation,⁸ miniaturization,⁹ and power efficiency.¹⁰ Thus, in recent years, most of the papers published on biofuel cells

[†] Clarkson University.

[‡] Department of Biotechnology Engineering, Ben-Gurion University of the Negev.

[§] Department of Chemistry, Ben-Gurion University of the Negev.

- (1) (a) Davis, F.; Higson, S. P. J. *Biosens. Bioelectron.* **2007**, *22*, 1224–1235. (b) Bullen, R. A.; Arnot, T. C.; Lakeman, J. B.; Walsh, F. C. *Biosens. Bioelectron.* **2006**, *21*, 2015–2045. (c) Shukla, A. K.; Suresh, P.; Berchmans, S.; Rajendran, A. *Curr. Sci.* **2004**, *87*, 455–468. (d) Katz, E.; Willner, I. In *Advanced Macromolecular and Supramolecular Materials and Processes*; Geckeler, K. E., Ed.; Kluwer Academic/Plenum Publishers: New York, 2003; pp 175–196. (e) Katz, E.; Shipway, A. N.; Willner, I. In *Handbook of Fuel Cells - Fundamentals, Technology, Applications*; Vielstich, W.; Gasteiger, H.; Lamm, A., Eds.; Wiley: 2003; Vol. 1, Part 4, Chapter 21, pp 355–381. (f) Katz, E. In *2004 Yearbook of Science and Technology*; Blumel, D., Ed.; McGraw-Hill Professional: New York, 2004; pp 33–37.
- (2) (a) Tasca, F.; Gorton, L.; Harreither, W.; Haltrich, D.; Ludwig, R.; Noll, G. *J. Phys. Chem. C* **2008**, *112*, 9956–9961. (b) Tasca, F.; Gorton, L.; Harreither, W.; Haltrich, D.; Ludwig, R.; Noll, G. *J. Phys. Chem. C* **2008**, *112*, 13668–13673. (c) Kuwahara, T.; Oshima, K.; Shimomura, M.; Miyauchi, S. *J. Appl. Polym. Sci.* **2007**, *104*, 2947–2953. (d) Sato, F.; Togo, M.; Islam, M. K.; Matsue, T.; Kosuge, J.; Fukasaku, N.; Kurosawa, S.; Nishizawa, M. *Electrochem. Commun.* **2005**, *7*, 643–647.

- (3) (a) Kavanagh, P.; Jenkins, P.; Leech, D. *Electrochem. Commun.* **2008**, *10*, 970–972. (b) Gallaway, J.; Wheelton, I.; Rincon, R.; Atanassov, P.; Banta, S.; Barton, S. C. *Biosens. Bioelectron.* **2008**, *23*, 1229–1235. (c) Nogala, W.; Rozniecka, E.; Zawisza, I.; Rogalski, J.; Opalio, M. *Electrochem. Commun.* **2006**, *8*, 1850–1854. (d) Mano, N.; Soukharev, V.; Heller, A. *J. Phys. Chem. B* **2006**, *110*, 11180–11187. (e) Farneth, W. E.; Diner, B. A.; Gierke, T. D.; D'Amore, M. B. *J. Electroanal. Chem.* **2005**, *581*, 190–196. (f) Tsujimura, S.; Kano, K.; Ikeda, T. *J. Electroanal. Chem.* **2005**, *576*, 113–120. (g) Tsujimura, S.; Kawaharada, M.; Nakagawa, T.; Kano, K.; Ikeda, T. *Electrochem. Commun.* **2003**, *5*, 138–141. (h) Palmore, G. T. R.; Kim, H. H. *J. Electroanal. Chem.* **1999**, *464*, 110–117.
- (4) (a) Cracknell, J. A.; Vincent, K. A.; Armstrong, F. A. *Chem. Rev.* **2008**, *108*, 2439–2461. (b) Minteer, S. D.; Liaw, B. Y.; Cooney, M. J. *Curr. Opin. Biotechnol.* **2007**, *18*, 228–234. (c) Liu, Q.; Xu, X. H.; Ren, G. L.; Wang, W. *Prog. Chem.* **2006**, *18*, 1530–1537. (d) Kim, J.; Jia, H. F.; Wang, P. *Biotechnol. Adv.* **2006**, *24*, 296–308.
- (5) (a) Lu, N.; Zhou, S. G.; Ni, J. R. *Prog. Chem.* **2008**, *20*, 1233–1240. (b) Du, Z. W.; Li, H. R.; Gu, T. Y. *Biotechnol. Adv.* **2007**, *25*, 464–482. (c) Yi, G.; Xin, Z. *Prog. Chem.* **2007**, *19*, 74–79. (d) Logan, B. E.; Regan, J. M. *Trends Microbiol.* **2006**, *14*, 512–518. (e) Logan, B. E.; Hamelers, B.; Rozendal, R.; Schrorder, U.; Keller, J.; Freguia, S.; Aelterman, P.; Verstraete, W.; Rabaey, K. *Environ. Sci. Technol.* **2006**, *40*, 5181–5192.

moved from journals covering fundamental chemical problems¹¹ to chemical and electrical engineering journals.¹² The present situation creates an illusion that this topic is no longer in the area of basic research. This paper uncovers a new area of fundamental research activity in biofuel cell studies: the coupling of biofuel cells with biocomputing systems to yield “smart” bioelectronic devices releasing energy on-demand upon processing biochemical information.

One of the important potential applications of the biofuel cells is powering of implantable biomedical devices.¹³ In this case a miniaturized biofuel cell must be implanted in a human body and use naturally existing biochemical substances as fuel (e.g., glucose in blood).¹⁴ Adaptive behavior of the implantable biofuel cell self-regulating the power release would be an immense advantage of these bioelectronic devices. Modified electrodes switchable between electrochemically active and inactive states by various physical and/or chemical signals were actively studied in the past decade,¹⁵ but very few of them were considered for their use in biofuel cells.¹⁶ It should be also noted that most of the developed switchable electrodes were activated/

deactivated by artificial signals (usually by light,¹⁷ magnetic field,¹⁸ or electrical potential¹⁹) applied to the systems, and they do not provide communication with their biochemical environment to regulate (switch or tune) the electrode activity according to the presence or absence of biochemical substances. A bioelectrocatalytic electrode, recently developed by us, demonstrated for the first time the switchable properties controlled by in situ biochemical reactions.²⁰ Specifically, the bioelectrocatalytic oxidation of glucose biocatalyzed by glucose oxidase and mediated by a redox polymer associated with the electrode

- (6) (a) Willner, I.; Katz, E. *Angew. Chem., Int. Ed.* **2000**, *39*, 1180–1218. (b) Katz, E.; Shipway, A. N.; Willner, I. In *Encyclopedia of Electrochemistry, Vol. 9: Bioelectrochemistry*; Wilson, G. S., Ed.; Bard, A. J., Stratmann, M. (Eds.-in-Chief); Wiley-VCH GmbH: Weinheim, Germany, 2002; Chapter 17, pp 559–626. (c) Rusling, J. F.; Forster, R. J. *J. Colloid Interface Sci.* **2003**, *262*, 1–15. (d) Heller, A. *J. Phys. Chem.* **1992**, *96*, 3579–3587. (e) Ghindilis, A. L.; Atanasov, P.; Wilkins, E. *Electroanalysis* **1997**, *9*, 661–674.
- (7) (a) Ivnitski, D.; Branch, B.; Atanasov, P.; Apblett, C. *Electrochem. Commun.* **2006**, *8*, 1204–1210. (b) Barriere, F.; Kavanagh, P.; Leech, D. *Electrochim. Acta* **2006**, *51*, 5187–5192. (c) Ramanavicius, A.; Kausaite, A.; Ramanaviciene, A. *Biosens. Bioelectron.* **2005**, *20*, 1962–1967. (d) Yuhashi, N.; Tomiyama, M.; Okuda, J.; Igarashi, S.; Ikebukuro, K.; Sode, K. *Biosens. Bioelectron.* **2005**, *20*, 2145–2150. (e) Mano, N.; Heller, A. *J. Electrochem. Soc.* **2003**, *150*, A1136–A1138. (f) Katz, E.; Willner, I.; Kotlyar, A. B. *J. Electroanal. Chem.* **1999**, *479*, 64–68.
- (8) (a) Pellissier, M.; Barriere, F.; Downard, A. J.; Leech, D. *Electrochem. Commun.* **2008**, *10*, 835–838. (b) Moehlenbrock, M. J.; Minter, S. D. *Chem. Soc. Rev.* **2008**, *37*, 1188–1196. (c) Kang, C.; Shin, H.; Heller, A. *Bioelectrochemistry* **2006**, *68*, 22–26.
- (9) (a) Li, X. C.; Zhou, H. J.; Yu, P.; Su, L.; Ohsaka, T.; Mao, L. Q. *Electrochem. Commun.* **2008**, *10*, 851–854. (b) Togo, M.; Takamura, A.; Asai, T.; Kaji, H.; Nishizawa, M. *Electrochim. Acta* **2007**, *52*, 4669–4674. (c) Lim, K. G.; Palmore, G. T. R. *Biosens. Bioelectron.* **2007**, *22*, 941–947. (d) Fischback, M. B.; Youn, J. K.; Zhao, X. Y.; Wang, P.; Park, H. G.; Chang, H. N.; Kim, J.; Ha, S. *Electroanalysis* **2006**, *18*, 2016–2022. (e) Kjeang, E.; Sinton, D.; Harrington, D. A. *J. Power Sources* **2006**, *158*, 1–12. (f) Moore, C. M.; Minter, S. D.; Martin, R. S. *Lab Chip* **2005**, *5*, 218–225. (g) Mano, N.; Mao, F.; Heller, A. *ChemBioChem* **2004**, *5*, 1703–1705. (h) Heller, A. *Phys. Chem. Chem. Phys.* **2004**, *6*, 209–216. (i) Mano, N.; Mao, F.; Shin, W.; Chen, T.; Heller, A. *Chem. Commun.* **2003**, 518–519.
- (10) (a) Mano, N. *Chem. Commun.* **2008**, 2221–2223. (b) Liu, Y.; Dong, S. J. *Electrochem. Commun.* **2007**, *9*, 1423–1427. (c) Schroder, U. *Phys. Chem. Chem. Phys.* **2007**, *9*, 2619–2629. (d) Wilkinson, S.; Klar, J.; Applegarth, S. *Electroanalysis* **2006**, *18*, 2001–2007. (e) Ringeisen, B. R.; Henderson, E.; Wu, P. K.; Pietron, J.; Ray, R.; Little, B.; Biffinger, J. C.; Jones-Meehan, J. M. *Environ. Sci. Technol.* **2006**, *40*, 2629–2634. (f) Mano, N.; Mao, F.; Heller, A. *J. Electroanal. Chem.* **2005**, *574*, 347–357. (g) Mano, N.; Mao, F.; Heller, A. *Chem. Commun.* **2004**, *18*, 2116–2117.
- (11) (a) Mano, N.; Fernandez, J. L.; Kim, Y.; Shin, W.; Bard, A. J.; Heller, A. *J. Am. Chem. Soc.* **2003**, *125*, 15290–15291. (b) Chaudhuri, S. K.; Lovley, D. R. *Nat. Biotechnol.* **2003**, *21*, 1229–1232. (c) Mano, N.; Mao, F.; Heller, A. *J. Am. Chem. Soc.* **2003**, *125*, 6588–6594. (d) Katz, E.; Lioubashevski, O.; Willner, I. *J. Am. Chem. Soc.* **2005**, *127*, 3979–3988. (e) Mao, F.; Mano, N.; Heller, A. *J. Am. Chem. Soc.* **2003**, *125*, 4951–4957. (f) Fernandez, J. L.; Mano, N.; Heller, A.; Bard, A. J. *Angew. Chem., Int. Ed.* **2004**, *43*, 6355–6357. (g) Soukharev, V.; Mano, N.; Heller, A. *J. Am. Chem. Soc.* **2004**, *126*, 8368–8369. (h) Mano, N.; Mao, F.; Heller, A. *J. Am. Chem. Soc.* **2002**, *124*, 12962–12963. (i) Katz, E.; Buckmann, A. F.; Willner, I. *J. Am. Chem. Soc.* **2001**, *123*, 10752–10753.
- (12) (a) Okuda-Shimazaki, J.; Kakehi, N.; Yamazaki, T.; Tomiyama, M.; Sode, K. *Biotechnol. Lett.* **2008**, *30*, 1753–1758. (b) Merle, G.; Brunel, L.; Tingry, S.; Cretin, M.; Rolland, M.; Servat, K.; Jolival, C.; Innocent, C.; Seta, P. *Mater. Sci. Engin. C* **2008**, *28*, 932–938. (c) Torres, C. I.; Marcus, A. K.; Rittmann, B. E. *Biotechnol. Bioeng.* **2008**, *100*, 872–881. (d) Jeon, S. W.; Lee, J. Y.; Lee, J. H.; Kang, S. W.; Park, C. H.; Kim, S. J. *Ind. Eng. Chem.* **2008**, *14*, 338–343. (e) Smolander, M.; Boer, H.; Valkiainen, M.; Roozeman, R.; Bergelin, M.; Eriksson, J. E.; Zhang, X. C.; Koivula, A.; Viikari, L. *Enzyme Microbial Technol.* **2008**, *43*, 93–102. (f) Clauwaert, P.; Aelterman, P.; Pham, T. H.; De Schampelaire, L.; Carballa, M.; Rabaey, K.; Verstraete, W. *Appl. Microbiol. Biotechnol.* **2008**, *79*, 901–913. (g) Togo, M.; Takamura, A.; Asai, T.; Kaji, H.; Nishizawa, M. *J. Power Sources* **2008**, *178*, 53–58. (h) Bedekar, A. S.; Feng, J. J.; Krishnamoorthy, S.; Lim, K. G.; Palmore, G. T. R.; Sundaram, S. *Chem. Eng. Commun.* **2008**, *195*, 256–266. (i) Arechederra, R. L.; Treu, B. L.; Minter, S. D. *J. Power Sources* **2007**, *173*, 156–161. (j) Tamaki, T.; Yamaguchi, T. *Ind. Eng. Chem. Res.* **2006**, *45*, 3050–3058.
- (13) Barton, S. C.; Gallaway, J.; Atanasov, P. *Chem. Rev.* **2004**, *104*, 4867–4886.
- (14) Heller, A. *Anal. Bioanal. Chem.* **2006**, *385*, 469–473.
- (15) (a) Pita, M.; Katz, E. *Electroanalysis* **2008**, in press. (b) Katz, E.; Willner, B.; Willner, I. *Biosens. Bioelectron.* **1997**, *12*, 703–719. (c) Motornov, M.; Sheparovych, R.; Katz, E.; Minko, S. *ACS Nano* **2008**, *2*, 41–52. (d) Flood, A. H.; Ramirez, R. J. A.; Deng, W. Q.; Muller, R. P.; Goddard, W. A.; Stoddart, J. F. *Aust. J. Chem.* **2004**, *57*, 301–322.
- (16) Katz, E.; Willner, I. *J. Am. Chem. Soc.* **2003**, *125*, 6803–6813.
- (17) (a) Lion-Dagan, M.; Katz, E.; Willner, I. *J. Am. Chem. Soc.* **1994**, *116*, 7913–7914. (b) Katz, E.; Lion-Dagan, M.; Willner, I. *J. Electroanal. Chem.* **1995**, *382*, 25–31. (c) Willner, I.; Lion-Dagan, M.; Marx-Tibbon, S.; Katz, E. *J. Am. Chem. Soc.* **1995**, *117*, 6581–6592. (d) Willner, I.; Lion-Dagan, M.; Katz, E. *Chem. Commun.* **1996**, 623–624. (e) Doron, A.; Portnoy, M.; Lion-Dagan, M.; Katz, E.; Willner, I. *J. Am. Chem. Soc.* **1996**, *118*, 8937–8944. (f) Doron, A.; Katz, E.; Tao, G. L.; Willner, I. *Langmuir* **1997**, *13*, 1783–1790. (g) Liu, N. G.; Dunphy, D. R.; Atanasov, P.; Bunge, S. D.; Chen, Z.; Lopez, G. P.; Boyle, T. J.; Brinker, C. J. *Nano Lett* **2004**, *4*, 551–554. (h) Liu, Z. F.; Hashimoto, K.; Fujishima, A. *Nature* **1990**, *347*, 658–660.
- (18) (a) Hsing, I. M.; Xu, Y.; Zhao, W. T. *Electroanalysis* **2007**, *19*, 755–768. (b) Katz, E.; Baron, R.; Willner, I. *J. Am. Chem. Soc.* **2005**, *127*, 4060–4070. (c) Katz, E.; Sheeney-Haj-Ichia, L.; Basnar, B.; Felner, I.; Willner, I. *Langmuir* **2004**, *20*, 9714–9719. (d) Willner, I.; Katz, E. *Angew. Chem., Int. Ed.* **2003**, *42*, 4576–4588. (e) Katz, E.; Sheeney-Haj-Ichia, L.; Willner, I. *Chem. Eur. J.* **2002**, *8*, 4138–4148. (f) Hirsch, R.; Katz, E.; Willner, I. *J. Am. Chem. Soc.* **2000**, *122*, 12053–12054. (g) Wang, J.; Kawde, A. N. *Electrochem. Commun.* **2002**, *4*, 349–352. (h) Laocharoensuk, R.; Bulbarello, A.; Mannino, S.; Wang, J. *Chem. Commun.* **2007**, 3362–3364. (i) Wang, J. *Electroanalysis* **2008**, *20*, 611–615. (j) Loaiza, O. A.; Laocharoensuk, R.; Burdick, J.; Rodriguez, M. C.; Pingarron, J. M.; Pedrero, M.; Wang, J. *Angew. Chem., Int. Ed.* **2007**, *46*, 1508–1511. (k) Wang, J.; Scampicchio, M.; Laocharoensuk, R.; Valentini, F.; Gonzalez-Garcia, O.; Burdick, J. *J. Am. Chem. Soc.* **2006**, *128*, 4562–4563. (l) Lee, J.; Lee, D.; Oh, E.; Kim, J.; Kim, Y. P.; Jin, S.; Kim, H. S.; Hwang, Y.; Kwak, J. H.; Park, J. G.; Shin, C. H.; Kim, J.; Hyeon, T. *Angew. Chem., Int. Ed.* **2005**, *44*, 7427–7432.
- (19) (a) Zheng, L.; Xiong, L. *Colloids Surf. A* **2006**, *289*, 179–184. (b) Riskin, M.; Basnar, B.; Katz, E.; Willner, I. *Chem. Eur. J.* **2006**, *12*, 8549–8557. (c) Riskin, M.; Basnar, B.; Chegel, V. I.; Katz, E.; Willner, I.; Shi, F.; Zhang, X. *J. Am. Chem. Soc.* **2006**, *128*, 1253–1260. (d) Chegel, V. I.; Raitman, O. A.; Lioubashevski, O.; Shirshov, Y.; Katz, E.; Willner, I. *Adv. Mater.* **2002**, *14*, 1549–1553. (e) Le, X. T.; Jégou, P.; Viel, P.; Palacin, S. *Electrochem. Commun.* **2008**, *10*, 699–703.
- (20) Tam, T. K.; Zhou, J.; Pita, M.; Ornatka, M.; Minko, S.; Katz, E. *J. Am. Chem. Soc.* **2008**, *130*, 10888–10889.

surface was activated and then switched off by pH changes produced in situ by two biochemical reactions. The switchable behavior of the electrode was based on the pH-sensitive redox polymer, which was switched between redox active and inactive states upon pH-induced swelling and shrinking processes, respectively.²¹ Single biochemical signals were applied to activate and then switch off the bioelectrocatalytic oxidation of glucose at the modified electrode. However, the system complexity can be scaled up using a recently developed concept of enzyme logic gates processing multiple biochemical signals in the form of Boolean logic operations and producing an output signal dependent on all input signals and the logic program encoded in the enzyme-biocomputing system.²² Integration of two novel concepts: biochemically switchable electrodes and enzyme-based information processing systems would allow for switchable properties of a bioelectrode controlled by many biochemical signals appearing in situ. The present study demonstrates for the first time a switchable bioelectrode for bioelectrocatalytic reduction of oxygen and its integration into a biofuel cell resulting in the release of power controlled by multiple biochemical signals processed with Boolean logic.

Experimental Section

Chemicals and Materials. The enzymes for the bioelectrocatalytic electrodes and logic operations were obtained from Sigma-Aldrich and used without further purification: glucose oxidase (GOx) from *Aspergillus niger*, type X-S (EC 1.1.3.4); laccase (Lac) from *Trametes versicolor* (EC 1.10.3.2), glucose dehydrogenase (GDH) from *Pseudomonas* sp. (EC 1.1.1.47), amyloglucosidase (AGS) from *Aspergillus niger* (EC 3.2.1.3), esterase (Est) from porcine liver (EC 3.1.1.1), and urease (Ur) from jack beans (EC 3.5.1.5). Other chemicals purchased from Sigma-Aldrich or Fluka were analytical quality and used as supplied: 4,4'-dimethoxy-2,2'-bipyridine (dmo-bpy), (NH₄)₂OsCl₆, poly(4-vinylpyridine) (P4VP, MW 160 kDa), bromomethyldimethylchlorosilane, methylene blue, β-D-(+)-glucose, ethyl butyrate, maltose, β-nicotinamide adenine dinucleotide (NAD⁺), and urea. Ultrapure water (18.2 MΩ·cm⁻¹) from NANOpure Diamond (Barnstead) source was used in all of the experiments. ITO conductive glass (20 ± 5 Ω/sq) was purchased from Aldrich and used as an electrode material. Synthesis of Os(dmo-bpy)₂Cl₂ was performed according to the published procedure.²³ P4VP was functionalized with Os(dmo-bpy)₂ pendant groups in a solution, and then the redox polymer was grafted onto the ITO electrode surface according to the procedure published in details elsewhere.²¹ Briefly, the ITO electrode was reacted in toluene with 0.1% (v/v) bromomethyldimethylchlorosilane for 20 min at 70 °C. Then the silanized ITO glass was washed with toluene and then reacted with Os-complex-functionalized P4VP in toluene (10 mg·mL⁻¹) to yield the redox-modified electrode.

Electrochemical Measurements. Cyclic voltammetry measurements were performed with an ECO Chemie Autolab PSTAT 10 electrochemical analyzer using the software package GPES 4.9 (General Purpose Electrochemical System). The cyclic voltammetry was performed with a three-electrode system in a standard cell (ECO

Chemie), using the Os-P4VP-modified ITO as the working electrode (geometrical area 1.2 cm²), a Metrohm Pt wire as the counter electrode and a Metrohm Ag/AgCl/KCl 3 M as the reference electrode. All potentials reported in the paper are given vs this reference electrode. The biofuel cell was custom-made of two curved glass compartments (cathodic and anodic) with clamping ledges and Nafion membrane (0.09 mm thick, Alfa Aesar, CAS no. 66796-30-3) between them with the overall configuration of a "U"-shape. The voltage and current generated by the biofuel cell were measured by a multimeter (Meterman 37XR) using a variable resistance load. The measurements were carried out at ambient temperature (23 ± 2 °C).

Bioelectrocatalytic Electrodes in the Biofuel Cell. The Os-P4VP-modified ITO electrode (1.2 cm² geometrical area) was used to mediate laccase-biocatalyzed O₂ reduction. The enzyme (laccase) was applied in a solution (112 units·mL⁻¹) using 0.1 M sodium sulfate as a background electrolyte being under equilibrium with air. Air was being bubbled during pH adjustment and during additions of different substrates (not during measurements). In addition to the laccase biocatalytic system, the enzymes operating as the logic gates and reset were added to the solution in the cathode compartment (the compositions of the logic gates and the reset system are given below). A bare ITO electrode (1.2 cm² geometrical area) for the glucose oxidation was used in 0.1 M phosphate buffer, pH 7, solution containing GOx (250 units·mL⁻¹), methylene blue (0.1 mM), and glucose (100 mM). The glucose-oxidizing electrode operated under Ar.

Composition of Logic Gates and Input Signals. The OR gate "machinery" was defined as an aqueous solution including 0.1 M sodium sulfate, GOx (5 units·mL⁻¹), and Est (5 units·mL⁻¹). The additions of glucose, input A (2 mM), and ethyl butyrate, input B (4 mM), were used as the biochemical input signals processed by the enzyme OR logic gate. The AND gate "machinery" was defined as an aqueous solution including 0.1 M sodium sulfate, AGS (5 units·mL⁻¹), and GDH (5 units·mL⁻¹). The additions of maltose, input A (50 mM), and NAD⁺, input B (0.5 mM), were used as the biochemical input signals processed by the enzyme AND logic gate. To perform the Reset function each enzyme logic gate also included urease (10 units·mL⁻¹). The trigger for the Reset function was an input signal of urea (5 mM). All logic gates operated at room temperature and in equilibrium with air. All concentrations of the substrates mentioned above, and the amounts of the enzyme inputs were optimized to produce a significant ΔpH yielding clearly distinguishable "0" and "1" states.

Logic Gates Action. To record the logic gates action, the "machinery" solution of each system was monitored with a pH meter (SevenEasy, Mettler-Toledo Inc.) at room temperature. Being a nonbuffered solution, the system requires an equilibration time to achieve a constant pH value. This value was taken as (0,0) input. Chemical inputs A and B were added to the system in all different combinations (0,1; 1,0; 1,1) to get the results that correspond to the possible truth table combinations. The pH values were recorded continuously during the whole experiment. The same procedure was performed for the AND gate, the OR gate, and the Reset trigger. Cyclic voltammograms for the O₂-bioelectrocatalytic electrode and V-i output generated by the biofuel cell were recorded prior to the logic gate operations and after completion of the respective biochemical reactions.

Results and Discussion

The Os-P4VP-modified ITO electrode studied in detail earlier²¹ demonstrates the pH-switchable properties: the Os-complex redox species immobilized on the electrode surface are electrochemically active at pH < 4.5 (*E*^o = 0.29 V, pH = 4.0), while upon increasing pH above 5.5 the modified electrode does not show electrochemical activity related to their redox process. This was explained by the pH-controlled transition of the electrode-tethered polymer brushes between swollen (at pH

(21) Tam, T. K.; Ornatka, M.; Pita, M.; Minko, S.; Katz, E. *J. Phys. Chem. C* **2008**, *112*, 8438–8445.

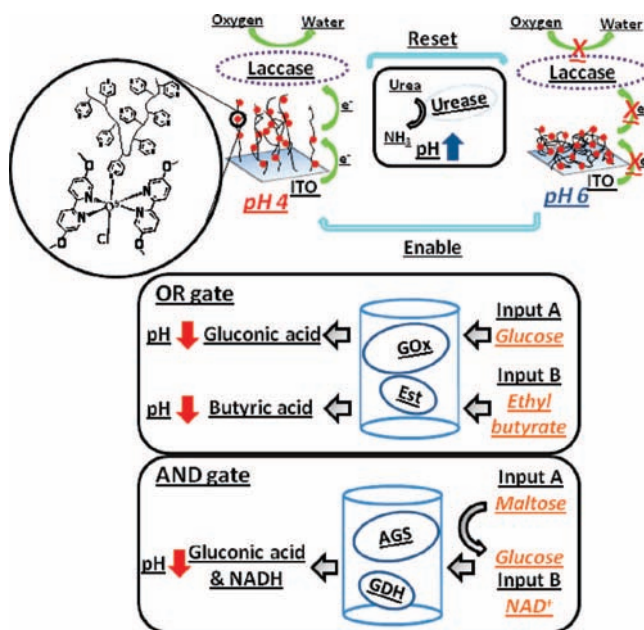
(22) (a) Strack, G.; Pita, M.; Ornatka, M.; Katz, E. *ChemBioChem* **2008**, *9*, 1260–1266. (b) Strack, G.; Ornatka, M.; Pita, M.; Katz, E. *J. Am. Chem. Soc.* **2008**, *130*, 4234–4235. (c) Niazov, T.; Baron, R.; Katz, E.; Lioubashevski, O.; Willner, I. *Proc. Natl. Acad. U.S.A.* **2006**, *103*, 17160–17163. (d) Baron, R.; Lioubashevski, O.; Katz, E.; Niazov, T.; Willner, I. *Org. Biomol. Chem.* **2006**, *4*, 989–991. (e) Baron, R.; Lioubashevski, O.; Katz, E.; Niazov, T.; Willner, I. *J. Phys. Chem. A* **2006**, *110*, 8548–8553. (f) Baron, R.; Lioubashevski, O.; Katz, E.; Niazov, T.; Willner, I. *Angew. Chem., Int. Ed.* **2006**, *45*, 1572–1576.

(23) Taylor, C.; Kenausis, G.; Katakis, I.; Heller, A. *J. Electroanal. Chem.* **1995**, *396*, 511–515.

< 4.5) and shrunken (at pH > 5.5) states. The hydrophilic swollen state generated upon protonation of the polymer pyridine units allows random quasidiffusional translocation of the polymer chains at the electrode surface resulting in short distances between the polymer-bound redox units and the conducting support favorable for the efficient electron transfer between them. Thus, the modified electrode shows a reversible cyclic voltammogram reflecting fast electron transport between the Os-complex and electrode support. Upon elevating the pH above 5.5, the pyridine units are deprotonated and the hydrophobic shrunken state of the polymer is generated. The electrochemical process of the Os-complex is inhibited because the polymer chains are “frozen” and their translocation essential for the electrochemical process is not possible. The reversible transition of the modified electrode between the electrochemically active and inactive states was already used to switch ON and OFF the bioelectrocatalytic glucose oxidation mediated by the redox polymer.²⁰ The pH changes controlling the electrode activity were produced in situ by enzyme reactions activated by the **Enable** and **Reset** biochemical signals. Still only a single biochemical signal was applied to activate the bioelectrocatalytic system and another single signal was used to shut it down.²⁰ In the present study we designed the enzyme systems performing Boolean logic operations **AND/OR** upon accepting two input signals and resulting in the pH changes controlling the activity of the bioelectrocatalytic system. In principle, the enzyme logic operations affecting the redox activity of the modified electrode could be coupled with any bioelectrocatalytic process mediated by the pH-switchable modified electrode, for example with the bioelectrocatalytic oxidation of glucose in the presence of GOx. However, we decided that the demonstration of the logically controlled bioelectrocatalytic reduction of oxygen would be the most interesting and challenging. Indeed, if the O₂-electrochemical reduction is logically controlled, it could be easily coupled with any bioelectrocatalytic anodic process (not only glucose oxidation) to yield a logically controlled biofuel cell. This approach would allow logically switchable enzyme-based as well as microbial biofuel cells using the same O₂-electrode integrated with the enzyme logic systems. To illustrate the concept, the developed logically controlled O₂-electrode was coupled with a simple bioelectrocatalytic anodic system composed of glucose and soluble GOx mediated by a diffusional redox relay, methylene blue.

The designed enzyme logic gates changing in situ pH values upon processing biochemical input signals and their coupling with the pH-switchable electrode are shown in Scheme 1. The **OR** logic gate was composed of two soluble enzymes: GOx (5 units·mL⁻¹) and Est (5 units·mL⁻¹). The system was under equilibrium with air and included O₂ as a natural electron acceptor for GOx. The enzyme system was activated by two biochemical input signals: glucose, input **A** (2 mM), and ethyl butyrate, input **B** (4 mM). The absence of glucose or ethyl butyrate was considered as the digital input signal “0”, while their presence in the operational concentrations was considered as the input signal “1”. The biocatalytic reactions in the presence of glucose and ethyl butyrate resulted in the formation of gluconic acid and butyric acid, respectively, both producing low pH values in the nonbuffered solution. Thus, in the presence of any substrate (input signals “0,1” or “1,0”) or both of them together (input signals “1,1”) one of the reactions or both of them proceeded and resulted in the acidification of the solution reaching pH = 4.2 ± 0.1, Figure 1A. The pH value was unchanged keeping the original value of pH ca. 6 only in the

Scheme 1. The pH-Switchable Bioelectrocatalytic Electrode for Oxygen Reduction Controlled by the Enzyme-Based **AND/OR** Logic Gates



absence of the both substrates (input signals “0,0”). Therefore, the features of the system corresponded to an **OR** logic operation. The **AND** logic gate was also composed of two soluble enzymes: AGS (5 units·mL⁻¹) and GDH (5 units·mL⁻¹). The system was also saturated with air for the biocatalytic reduction of oxygen by laccase. The enzyme system was activated by two biochemical input signals: maltose, input **A** (50 mM), and NAD⁺, input **B** (0.5 mM), participating in a two-step chain reaction. In the first step maltose was hydrolyzed by AGS to glucose, and then glucose was oxidized by GDH to gluconic acid. The second reaction required NAD⁺ as an electron acceptor and the chain reaction cannot be completed in the absence of NAD⁺ even if glucose was produced in the first step. The absence of maltose or NAD⁺ was considered as the digital input signal “0”, while their presence in the operational concentrations was considered as the input signal “1”. In the absence of any or both substrates (input signals “0,0”, “0,1”, or “1,0”) the two-step reaction chain was not completed and the pH value was not changed. In the presence of the both substrates (input signals “1,1”) the reaction proceeded until the very end, resulting in the formation of gluconic acid and acidification of the solution reaching pH = 4.4 ± 0.1, Figure 1B. Therefore, the features of the system corresponded to an **AND** logic operation. The kinetics of the pH changes generated in situ by the enzyme systems depends on the activity of the enzymes which is different in various systems (compare curves b and c–d in Figure 1A). After completion of the enzyme reactions resulting in the logically controlled acidic medium (pH = 4.1–4.5), the pH value can be reset to the initial value (pH ca. 6) by the formation of ammonia upon hydrolysis of urea biocatalyzed by urease (10 units·mL⁻¹), Scheme 1. Thus, the **Reset** function was activated by the input signal composed of urea (5 mM). A control experiment performed in the absence of the enzyme logic systems demonstrated no effect on the pH value from the added chemical input signals.

It should be noted that some of the logic gates composed of several enzymes could be simplified (including the **AND** logic gate used in the present paper). However, the major challenge

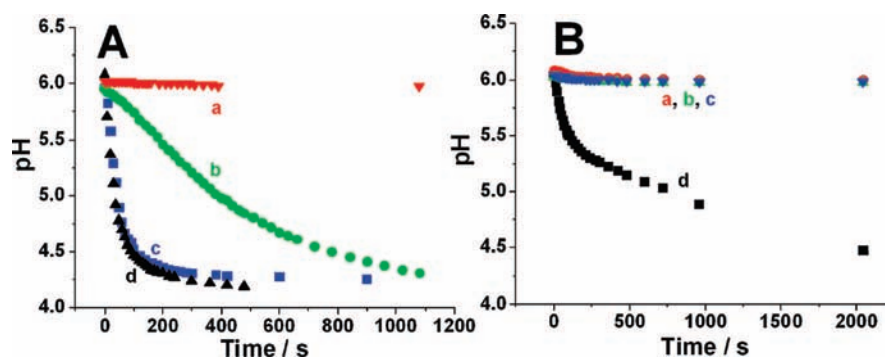


Figure 1. The pH changes observed in the solutions containing OR (A)/AND (B) logic gates operating according to Scheme 1 upon addition of different combinations of the biochemical input signals: (a) 0,0, (b) 1,0, (c) 0,1, and (d) 1,1. The exact composition of the enzyme logic gates and the definition of the biochemical signals are given in the Experimental Section.

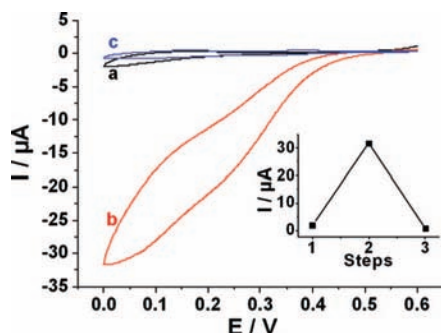


Figure 2. Cyclic voltammograms obtained on the Os–P4VP-modified ITO electrode at its active and inactive states in the presence of laccase ($22.4 \text{ units} \cdot \text{mL}^{-1}$) and O_2 (under equilibrium with air): (a) prior to the application of the biochemical input signals (pH ca. 6) when the modified electrode is inactive, (b) after the electrode was activated by changing pH to ca. 4.2 by the biochemical signals (combinations “1,0”, “0,1”, or “1,1” for the OR gate and “1,1” for the AND gate), (c) after the **Reset** function activated by the addition of 5 mM urea. The cyclic voltammograms were recorded at the potential scan rate of $10 \text{ mV} \cdot \text{s}^{-1}$. Inset shows the reversible activation of the bioelectrocatalytic O_2 reduction triggered by chemical signals.

in the enzyme logic (and in the biomolecular computing in general) is the possibility of scaling up the systems, resulting in logic networks mimicking natural pathways involving cooperative work of many enzymes. Specifically, in the present paper we used the **AND** gate operating with the use of two enzymes since it would allow future optimization of the gate performance.²⁴ Application of a single-enzyme logic gate, despite its simplicity, does not allow optimization of the information processing. The gate optimization was outside the scope of the present paper, but it is in process (theoretically and experimentally) in our laboratory and will be published elsewhere.

In addition to monitoring the pH changes, we recorded cyclic voltammograms on the Os–P4VP-modified ITO electrode upon applying different combinations of the input signals (note that O_2 and laccase, $22.4 \text{ units} \cdot \text{mL}^{-1}$, were always in the solution). The experiments were always started at pH ca. 6, when the redox polymer on the electrode surface is in the shrunken state and is not electrochemically active. The cyclic voltammogram recorded at this pH shows the mute state of the electrode when there is no reduction of O_2 in the system, Figure 2, curve a. If the enzyme-catalyzed reactions upon appropriate combinations of the input signals are activated and the acidic medium is produced, the redox polymer transforms to the electrochemically

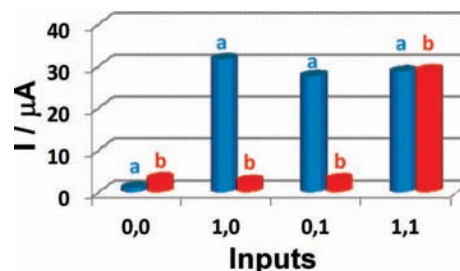


Figure 3. The bar diagram showing the bioelectrocatalytic current of O_2 reduction (derived from the cyclic voltammograms at $E = 0.0 \text{ V}$) as the logic function of different combinations of the biochemical input signals: (a) OR logic gate, (b) AND logic gate.

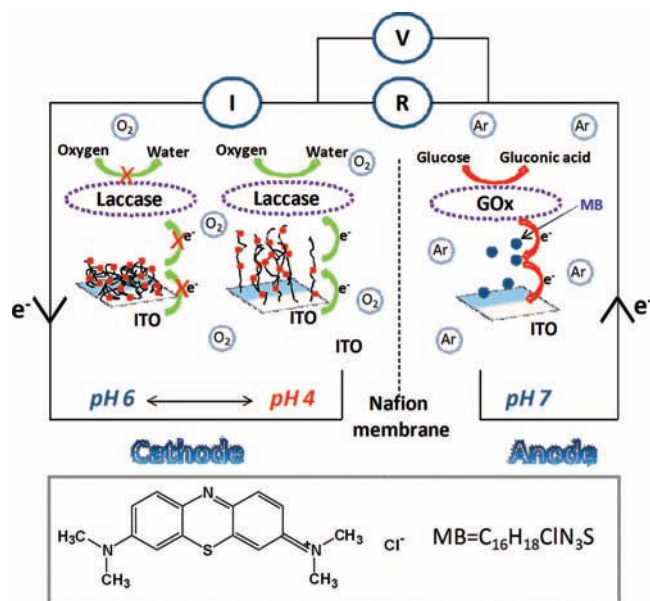
active swollen state, Scheme 1, and the bioelectrocatalytic cathodic wave corresponding to O_2 reduction is observed on the cyclic voltammogram, Figure 2, curve b. The bioelectrocatalytic cathodic wave of the O_2 reduction starts at ca. 0.47 V that corresponds to the beginning of the cathodic wave of the immobilized Os-complex²¹ operating as the electron transfer mediator. When the **Reset** function was activated by addition of urea and therefore the pH returned to an almost neutral value, a cyclic voltammogram was recorded, showing that the system returned to the mute state of the electrochemical system, Figure 2, curve c. The reversible cycle between inactive–active–inactive states was achieved upon introducing specific biochemical signals into the system, Figure 2, inset. However, the most important features of the system are shown in Figure 3 where the bioelectrocatalytic current developed in the system is depicted as a function of the input signal combinations. When the enzyme **OR** logic system was used, the bioelectrocatalytic current corresponding to the O_2 reduction was activated at three combinations of the input signals “0,1”, “1,0”, or “1,1”, reflecting the truth table characteristic of the **OR** Boolean logic operation. The bioelectrocatalytic O_2 cathodic wave was observed in the presence of the enzyme **AND** logic system when only “1,1” set of the signals was applied, reflecting the truth table characteristic of the **AND** Boolean logic operation.

The logically controlled O_2 reducing bioelectrode was coupled with a glucose-oxidizing bioelectrocatalytic system to yield a biofuel cell, Scheme 2. The bioelectrochemical oxidation of glucose (100 mM) in the presence of soluble GOx ($250 \text{ units} \cdot \text{mL}^{-1}$) and methylene blue (0.1 mM) operating as a diffusional electron transfer mediator²⁵ was selected as the simplest example of an anodic reaction to demonstrate the

(24) Privman, V.; Strack, G.; Solenov, D.; Pita, M.; Katz, E. *J. Phys. Chem. B* **2008**, *112*, 11777–11784.

(25) Bartlett, P. N.; Tebbutt, P.; Whitaker, R. C. *Prog. React. Kinet.* **1991**, *16*, 55–155.

Scheme 2. The Biofuel Cell Composed of the pH-Switchable Logically Controlled Biocatalytic Cathode and Glucose-Oxidizing Anode



logically switchable biofuel cell. The system shows a well defined anodic bioelectrocatalytic wave corresponding to the glucose oxidation (see the cyclic voltammogram in the Supporting Information, Figure S11, curve b). The anodic wave corresponding to the bioelectrocatalytic oxidation of glucose starts at ca. -0.25 V that correlates with the redox potential of methylene blue ($E^\circ = -0.22$ V, pH = 7) which operates as the electron transfer mediator. The bioelectrocatalytic anodic process proceeds at potentials ca. 600–700 mV more negative than the reduction of O_2 , thus allowing the assembly of a biofuel cell. The anodic compartment containing the glucose-oxidizing bioelectrocatalytic system in 0.1 M phosphate buffer, pH 7, under argon was separated from the cathodic switchable O_2 electrode by a Nafion membrane, preventing mixing of the cathodic and anodic solutions. The cathodic compartment in addition to the O_2 reducing system (laccase in the solution, 112 units \cdot mL $^{-1}$, and the Os-complex electron relay at the electrode surface) included also the enzyme logic/reset system. In case of the **OR** logic/**Reset** system the solution contained GOx (5 units \cdot mL $^{-1}$), Est (5 units \cdot mL $^{-1}$) and urease (10 units \cdot mL $^{-1}$). The **OR** logic operation was activated by glucose (2 mM) and/or ethyl butyrate (4 mM) and then the **Reset** was activated by the addition of urea (5 mM). In case of the **AND** logic/**Reset** system the solution contained AGS (5 units \cdot mL $^{-1}$), GDH (5 units \cdot mL $^{-1}$) and urease (10 units \cdot mL $^{-1}$). The **AND** logic operation was activated by maltose (50 mM) and NAD^+ (0.5 mM), and then the **Reset** was activated by the addition of urea (5 mM). A nonbuffered solution of Na_2SO_4 , 0.1 mM, was used as a background electrolyte to facilitate the enzyme-induced pH changes. The experiments were always started at pH ca. 6 in the cathodic compartment when the biocathode is inactive, and then different combinations of the biochemical input signals were applied to activate the enzyme logic gates, to change in situ the pH value and to activate the biofuel cell. The V-i (voltage vs current density) polarization function of the biofuel cell was obtained upon application of variable load resistances and by measuring the current and voltage generated on them, Figure 4A. The power density produced by the biofuel cell upon connecting to the variable resistances was derived from the V-i

measurements, Figure 4B (another plot showing the power density vs the current density is shown in the Supporting Information, Figure S12). When the **OR** logic gate was applied with “0,0” input signals or the **AND** logic gate was used with “0,0”, “0,1”, or “1,0” input signals, the initial pH value of the solution was not changed and the biocatalytic cathode was inactive, thus resulting in the mute state of the biofuel cell. The V-i function of the biofuel cell in its mute state reveals ca. 80 mV for the open circuit voltage, V_{oc} , and $0.3 \mu A \cdot cm^{-2}$ for the short circuit current density, i_{sc} , Figure 4A, curve a. The maximum released power density, $P_{max} = 6 nW \cdot cm^{-2}$, was observed at the external load resistance of 290 k Ω , Figure 4B, curve a. The biofuel cell was activated when the **OR** logic gate was used and “0,1”, “1,0”, or “1,1” input signals were applied or when the **AND** logic gate was used and “1,1” input signals were applied. When the biofuel cell was activated (through activating the biocatalytic cathodic process), the V-i function was dramatically changed, demonstrating ca. 380 mV for the open circuit voltage, V_{oc} , and $3 \mu A \cdot cm^{-2}$ for the short circuit current density, i_{sc} , Figure 4A, curve b. The maximum power density was greatly increased, reaching $700 nW \cdot cm^{-2}$ at the external load resistance of 80 k Ω , Figure 4B, curve b. After the biofuel cell was activated by the enzyme logic operations and the cell characteristics were measured, the **Reset** function was applied by the addition of urea (5 mM) to return the pH to the initial value and to switch OFF the biofuel cell. When the initial pH was restored, the V-i function was measured again, and it showed a small voltage/current similar to that at the beginning of the experiment, Figure 4A, curve c. Obviously, the power released by the biofuel cell dropped to the initial low value, Figure 4B, curve c. The whole cycle which includes the logically processed activation of the biofuel cell and then reset resulting in its switch OFF can be followed by the reversible changes of V_{oc} and P_{max} , Figures 4A,B, insets. A small difference in the biofuel cell activity before its activation and after the reset function originates from slightly different pH values controlling the activity of the switchable interface. Figure 5 shows the logic control of the power produced by the biofuel cell, demonstrating the **AND/OR** logic switches upon application of different combinations of the biochemical input signals. The reproducibility of the experimental data (voltage, current, and power output) upon repeating the measurements was within $\pm 5\%$ depending on minor variations of the pH values controlling the interfacial activity.

It should be noted that the load resistance corresponding to the maximum power release was also reversibly changed between high (290 k Ω) and low (80 k Ω) values for the inactive and active states of the biofuel cell. One should remember that the external load resistance corresponding to the maximum power release is equal to the internal resistance of the biofuel cell (known as the impedance matching theorem in electrical circuits).²⁶ Thus, the change of the resistances reflects the variation of the internal properties of the bioelectrochemical system. The observed change of the resistance corresponds to the change of the interfacial electron transfer resistance of the bioelectrocatalytic cathode when it alternates between the mute and active states. It should be noted that even in the “mute” state (at pH ca. 6) the biofuel cell is producing some current and voltage. The current generated in the OFF state of the biofuel cell is 1 order of magnitude lower than that in the ON state, while V_{oc} in the “mute” state is ca. 20% of V_{oc} produced

(26) Crompton, T. R. *Battery Reference Book*, 3rd ed.; Elsevier: Oxford, 2000.

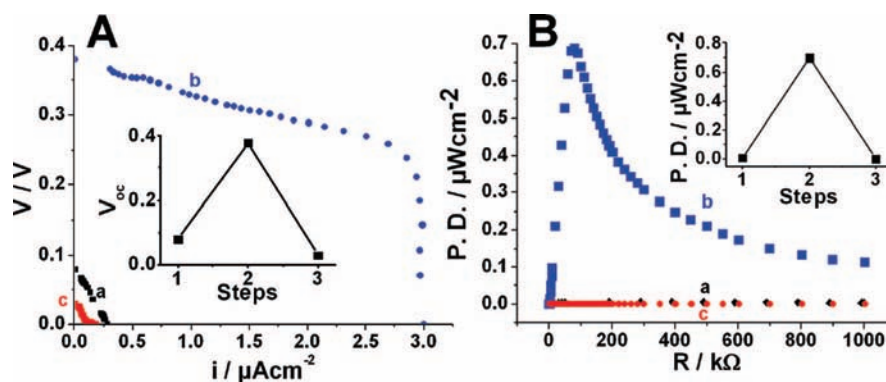


Figure 4. V-i polarization curves obtained for the biofuel cell with different load resistances (A) and the power density as a function of the resistance load (B): (a) in the inactive state prior to the addition of the biochemical input signals (pH value in the cathodic compartment ca. 6), (b) in the active state after the cathode was activated by changing pH to ca. 4.2 by the biochemical signals (combinations “1,0”, “0,1”, or “1,1” for the OR gate and “1,1” for the AND gate), (c) after the **Reset** function activated by the addition of 5 mM urea. Insets: Switchable V_{oc} (A) and power density (B) upon transition of the biofuel cell from the mute state to the active state and back, performed upon biochemical signals processed by the enzyme logic systems.

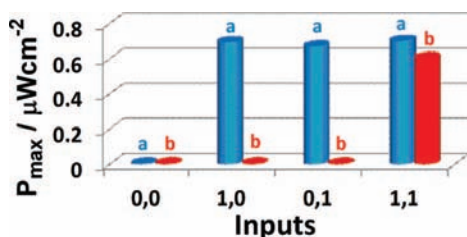


Figure 5. The bar diagram showing the power density obtained from the biofuel cell as the logic function of different combinations of the biochemical input signals: (a) OR logic gate, (b) AND logic gate.

by the active state of the cell. This originates from the fact that the bioelectrocatalytic cathode in its switched OFF state has a large barrier for the electron transfer process inhibiting the current formation, however, allowing formation of the potential difference at steady-state conditions.

Conclusions and Perspectives

The developed switchable biofuel cell activated by external biochemical signals logically processed by enzymatic systems is the first example of a bioelectronic device coupled with a biocomputing system. Such devices will provide a new dimension in bioelectronics and biocomputing benefiting from the integration of both concepts. The first example is obviously aiming only at the demonstration of this concept and still requires significant engineering efforts prior to a potential practical application. The following steps must be made to develop a real implantable device operating according to the immediate physiological needs and releasing electrical power on-demand: (i) the enzyme biocomputing systems should be integrated with biocatalytic electrodes rather than used in a solution. Application of immobilized enzymes operating as logic elements will allow multiple activation–deactivation cycles controlled by the enzyme logic. The first examples of enzyme logic gates with the electrode-immobilized enzymes are already available.²⁷ (ii) The biochemical input signals used to control the power production in the biofuel cell should have biological/medical importance, and they should be used at physiological concentrations. (iii) The complexity of the biocomputing system, which controls the biofuel cell, should be increased from a single Boolean operation (for example AND/OR) to a complex multicomponent/multifunctional logic network. This network will provide efficient

processing of multisignal information from the human body to adjust accordingly the power release from the implanted biofuel cell. The first steps in assembling^{22b,c} and optimization²⁴ of the logic networks composed of various concatenated logic gates were already published. Further development of sophisticated enzyme-based biocomputing networks will be an important phase in the development of “smart” bioelectronic devices. (iv) Obviously, the optimized electrical parameters, efficiency, durability, renewability, and miniaturization of the biofuel cell should be addressed. These aspects of the work are outside the scope of the present research which is at the moment concentrated on the coupling of a biofuel cell (as an example of a bioelectronic device) with a biocomputing system processing biochemical information. The present example of the biofuel cell coupled with the enzyme logic systems represents one of the facets of our multidisciplinary research program addressing, in general, biomolecular computing systems and their integration with electronic transducers and signal-responsive materials.²⁸

Acknowledgment. This research was supported by the NSF grants “Signal-Responsive Hybrid Biomaterials with Built-in Boolean Logic” (DMR-0706209) and “Biochemical Computing: Experimental and Theoretical Development of Error Correction and Digitalization Concepts” (CCF-0 726698). An award from the Semiconductor Research Corporation: “Cross-disciplinary Semiconductor Research” (No. 2008-RJ-1839G) is gratefully acknowledged. T.K.T. gratefully acknowledges the Wallace H. Coulter scholarship from Clarkson University. This research was also supported by the Converging Technologies program of the Israel Science Foundation (grant no. 1693/07) L.A. and M.M.M.

Supporting Information Available: The cyclic voltammogram of the glucose-oxidizing biocatalytic anode used in the biofuel cell and the plot showing the power density vs the current density. This material is available free of charge via the Internet at <http://pubs.acs.org>.

JA8076704

(28) (a) Pita, M.; Krämer, M.; Zhou, J.; Poghosian, A.; Schöning, M. J.; Fernández, V. M.; Katz, E. *ACS Nano* **2008**, *2*, 2160–2166. (b) Pita, M.; Minko, S.; Katz, E. *J. Mater. Sci.: Mater. Med.* **2008**, in press (DOI, 10.1007/s10856-008-3579-y). (c) Motornov, M.; Zhou, J.; Pita, M.; Gopishetty, V.; Tokarev, I.; Katz, E.; Minko, S. *Nano Lett.* **2008**, in press.

(27) Pita, M.; Katz, E. *J. Am. Chem. Soc.* **2008**, *130*, 36–37.